Kinetics of hexane pyrolysis at very high pressures. 1. Experimental study. Energy Fuels 3: 89-96

ARTICLE *in* ENERGY & FUELS · JANUARY 1989

Impact Factor: 2.79 · DOI: 10.1021/ef00013a016

1 AUTHOR:

Florent Domine
Laval University
154 PUBLICATIONS **3,987** CITATIONS

Kinetics of Hexane Pyrolysis at Very High Pressures. 1. Experimental Study†

Florent Dominé‡

CNRS, ER 224, Département de Géologie, Ecole Normale Supérieure, 46 rue d'Ulm, 75230 Paris Cedex 05, France

Received October 29, 1986. Revised Manuscript Received August 20, 1988

Pyrolysis of supercritical hexane (T_C = 234 °C, P_C = 29.3 bar) has been performed in a closed, constant-pressure gold reactor in the 210–15600-bar pressure range at 290–365 °C. Interest is focused on products formed at low (<2%) conversion, which are analyzed and identified by GC-MS. Reaction products are light alkanes from C_1 to C_5, light alkenes from C_2 to C_5, and heavy alkanes from C_8 to C_{12}. The formation of light products is explained by conventional chain reactions terminated by the recombination of hexyl radicals, while the formation of heavy alkanes results from the addition of hexyl radicals to alkenes. A quantitative treatment performed on a simplified mechanism shows that results obtained at 210 bar are in reasonable agreement with existing gas-phase data. As pressure is increased, relative light product yields, especially those of alkenes, decrease while those of heavy products increase. This can be interpreted mainly by considering the activation volumes of the reactions involved. It is predicted that the overall reaction rate decreases with pressure. Some possible geochemical implications are discussed.

Introduction

Crude oils are complex mixtures made up chiefly of hydrocarbons. These oils undergo thermal degradation in their rock reservoir. The accurate quantitative prediction of these thermally induced transformations can be of considerable economic importance. Numerous authors (see for example Tissot and Espitalié,[1] Ungerer,[2] and Burnham and Braun[3]) have therefore attempted to elaborate quantitative models accounting for the transformations observed in crude oils. These models are mainly empirical, and even though they have been found to be applicable to many natural cases, their theoretical basis is often questionable. For example, the chemical reactions used to describe the thermal evolution of organic matter are often global reactions that are the result of several elementary reactions. It is extremely likely that the relative importance of these elementary reactions will vary with pressure and temperature. The use of Arrhenius type kinetic parameters over a wide temperature range for such global reactions can lead to large quantitative errors, as already suggested by Snowdon.[4] Indeed, an elementary reaction can control the rate of the global reaction over a certain temperature range, while another elementary reaction with different Arrhenius parameters can control the overall reaction rate outside of that range. Also, pressure has remained a widely neglected parameter. Burnham and Braun[3] did consider quantitatively the effect of pressure in their model. However, the pressure dependence of their oil cracking results is empirical and cannot be extrapolated beyond their narrow low-pressure range. Limited data are also available on the effect of pressure on pure hydrocarbon pyrolysis. High-temperature (400–700 °C) data on pure compounds[5–7] show that pressure affects both product distribution and overall reaction rate. Some recently acquired data on complex organic matter evolved in high-pressure geological settings also suggests that pressure has important effects.[8] These data show that the effect of high pressure on hydrocarbon pyrolysis need to be investigated in detail in order to enable the prediction of the high-pressure thermal evolution of organic matter of geological interest.

As a first step towards a better understanding of the kinetic phenomena involved during the thermal evolution of complex hydrocarbon mixtures, an oversimplified system consisting of pure hexane has been pyrolyzed between 210 and 15 600 bar and 290 and 365 °C. The pressure range studied includes the pressures at which just about all known crude oil reservoirs evolve: according to Tissot and Welte,[9] petroleum can be found at depths of up to 7 km, at a pressure of about 1580 bar. It is detailed in The Effect of Pressure section why pressures higher than those found in geological settings need to be investigated here if future geochemical applications are planned. The temperature range studied has been chosen so that reaction time remains compatible with both the experimental system used (experiments must last at least 14 h) and a reasonably long reaction time (1 month).

Experimental and Analytical Methods

Normal hexane (n-C_6H_{14})has been pyrolyzed in a closed reactor consisting of a sealed gold tube. Gold was chosen as one of the most chemically inert metals.[10] Gold tubes were sealed at one end, then filled with Fluka 99.8% pure hexane under an argon atmosphere to avoid the presence of oxygen, and then arc welded at the other end. The system used is similar to that described in Favre et al.[11]

Experiments up to 4000 bar were carried out in cold seal autoclaves as shown in Figure 1. Gold tubes were 40 mm long by

† Work supported in part by the CNRS and in part by Institut Français du Pétrole Grant No. 8456.

‡ Present address: National Oceanic and Atmospheric Administration, R/E/AL2, 325 Broadway, Boulder, CO 80303.

(1) Tissot, B. P.; Espitalié, J. *Rev. Inst. Fr. Pet.* **1975**, *30*, 743–777.
(2) Ungerer, P. In *Thermal Phenomena in Sedimentary Basins*; Durand, B., Ed.; Technip: Paris, 1984; pp 235–246.
(3) Burnham, A. K.; Braun, R. L. *In Situ*, **1985**, *9*, 1–23.
(4) Snowdon, L. R. *AAPG Bull.* **1979**, *63*, 1128–1134.
(5) Voge, H. H.; Good, G. M. *J. Am. Chem. Soc.* **1949**, *71*, 593–597.
(6) Fabuss, B. M.; Smith, J. O.; Satterfield, C. N. *Adv. Pet. Chem. Refin.* **1964**, *9*, 157–201.
(7) Doué, F.; Guiochon, G. *J. Chim. Phys.* **1968**, *65*, 395–409.
(8) Goffé, B.; Villey, M. *Bull. Mineral.* **1984**, *107*, 81–91.
(9) Tissot, B. P.; Welte, D. H. *Petroleum Formation and Occurrence*; Springer Verlag: Berlin, Heidelberg, FRG, New York, 1978.
(10) Puddephatt, R. J. *The Chemistry of Gold*; Elsevier: New York, 1978; p 253.
(11) Favre, A.; Boulet, R.; Behar, F. *Rev. Inst. Fr. Pet.* **1985**, *40*, 609–623.

0887-0624/89/2503-0089$01.50/0

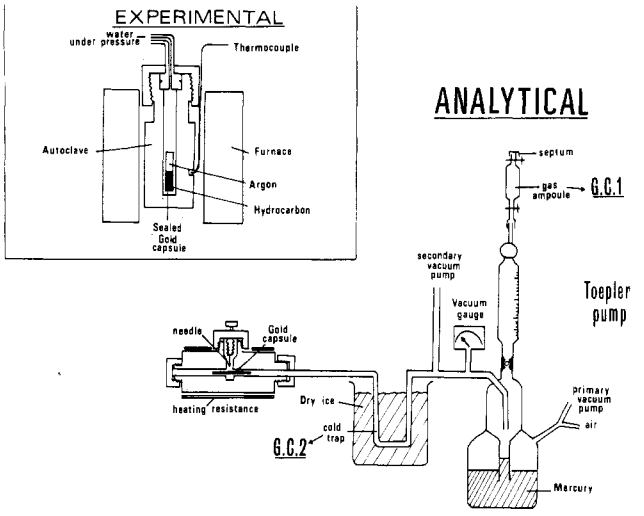

Figure 1. High-pressure apparatus used for experimentation and the analytical system used.

3.8 mm in diameter and were 0.2 mm thick. They contained 100–150 μL of hexane. Presure was transmitted by water (see Tuttle[12] for details). Pressure was measured within ±1% by an electronic manometer. PID electronic temperature regulators kept temperature within 1 °C of the specified temperature, which was measured to ±1% with a chromel–alumel thermocouple placed in a hole on the outer surface of the autoclave. After calibration, the appropriate temperature corrections were made to obtain the actual sample temperature. However, due to radial and longitudinal temperature gradients in the autoclave, an overall temperature accuracy no better than ±7 °C can be claimed.

Experiments at 15 600 bars were carried out in a piston cylinder apparatus as described in Mirwald et al.[13] Gold tubes were 16 mm long by 3 mm in diameter and contained 20 μL of hexane. They were placed in a pyrophillite/NaCl cell, and due to friction, actual pressure was somewhat lower than measured pressure, both values being different by less than 8%. Temperature accuracy for this system was ±5 °C. These 15 600-bar experiments were carried out at the Institut für Mineralogie, Ruhr Universität, Bochum, F.R.G.

The analytical apparatus is shown in Figure 1. The gold tube was placed in a vacuum cell heated to 105 °C similar to that described by Favre et al.[11] Residual pressure in the cell was below 10^{-6} bar. After the extraction line was isolated from the vacuum pump, the gold tube was pierced with a needle.

Condensable products (C_6–C_{18}) were cold trapped at −78 °C. These products were retrieved by rinsing the trap with pentane and then analyzed by GC or GC–MS. Products were separated on a 50-m capillary column with an apolar phase and detected with a flame-ionization detector. Electron-impact quadrupole MS was used for peak identification.

Uncondensable products (C_1-C_5) were compressed in a gas ampule by a Toeppler pump. Gas volume was measured in the calibrated part of the pump. Gas pressure was measured by the difference in mercury level between the calibrated part of the pump and another part under vacuum. The number of moles of gas was calculated by using the $PV = nRT$ relationship. A gastight syringe was used to inject the gas into a 10-μL sample loop. A 50-m capillary column with a KCl deactivated alumina phase was used to separate gaseous products.

In order to measure the amounts of molecular hydrogen (H_2) produced, two experiments were performed in the same autoclave at 1810 bar, 357 °C for 167 h. The cold trap was cooled in liquid N_2, so that only H_2 and CH_4 were not condensed in the trap, together with trace amounts of C_2H_6 and C_2H_4, as shown by the gas chromatograms of these mixtures, and probably also some trace amounts of argon. This gas mixture was retrieved in a gas ampule as usual. The ampule was then connected to a magnetic mass spectrometer with 24 collectors, detecting mass/charge ratios of 1–40. Hydrogen was quantified on the mass 2 collector, and CH_4 was quantified on the mass 15 collector. C_2H_6 and C_2H_4 contributions to mass 15 were indeed negligible in this case.

Results

Gas chromatograms of the uncondensable fraction (from now on referred to as light products) and of the condensable fraction (heavy products) are shown in Figure 2. Products do not vary qualitatively over the experimental range studied. Quantitatively, some ratios between products do not show much variation throughout this study: the main saturated light hydrocarbons are CH_4, C_2H_6, C_3H_8, and n-C_4H_{10} with approximate relative molar yields of 7:20:16:1. Light unsaturated hydrocarbons are C_2H_4, C_3H_6, and 1-C_4H_8 with average approximate relative yields of 1:20:5. For the two experiments where it has been measured, H_2:CH_4 ratios are 1.7×10^{-2} and 2×10^{-2}, which shows that H_2 is formed in negligible amounts. Heavy products (all of them saturated hydrocarbons) come with essentially three isomers of saturated C_8, C_9, C_{10}, C_{11}, and six C_{12} isomers. Relative yields for the main three C_{8-11} isomers are such that the ethyl-branched C_{x-2}:methyl-branched C_{x-1}:n-C_x ratio is close to 2:4:1. Moreover, the ratios C_9:C_{10}:C_{11} is close to 20:15:3. Other C_9, C_{10}, and C_{11} isomers are observed, mainly at the higher pressures studied. Their exact structure could not be determined; mass spectrometry just showed that, in general, they are more substituted than the identified isomers.

Ratios between the various classes of products just mentioned (light saturates, light unsaturates, C_8–C_{11}, C_{12}) show some significant variations with temperature and pressure. To give an idea of product yields, a product yield versus conversion plot is shown in Figure 3 for experiments at 210 bar and 357 °C. Products representative of each class are reported. Due to the large error in temperature (±7 °C), a product yield versus time plot would be meaningless, since it is found that the overall reaction rate doubles every 5–6 °C.

To investigate the effect of pressure, experiments have been carried out at 210, 1810, 3800, and 15 600 bar. In Figure 4 molar yields (i.e. 100 × mol of products/initial mol of reactant) of compounds representative of each product class has been plotted against pressure, at 357 °C and at 0.5% conversion. With increasing pressure, the following observations can be made. Light unsaturates production (C_2H_4, C_3H_6, 1-C_4H_8) is all but stopped at pressures above 5000 bar. Light saturates yields decrease dramatically. C_8–C_{11} yields increase slightly; this increase is greater for the heavier products of this class and is within experimental error for some products. The yields of 4-ethyloctane double over the pressure range investigated. C_{12} yields are greatly increased. Due to the ±7 °C accuracy in the temperature measurements, hexane consumption dependence on pressure is within experimental error.

To investigate the effect of temperature, experiments have been carried out at 290, 305, 335, 357 and 365 °C, at 210 bar. Figure 5 is an Arrhenius plot of the sum of the concentrations of all C_8–C_{11} over the concentration of C_6H_{14} multiplied by time. The point at 290 °C is surprising. This may be because these experiments have been performed in an autoclave different from all the others. In any case, this point should be discarded. A least-squares fit of the other four points yields an equation with Arrhenius parameters log (A, s^{-1}) = 27.83 and E = 103.1 kcal·mol^{-1}. Similarly, light product concentrations over the square root of the concentration of C_6H_{14} multiplied by time have been plotted against inverse temperature for the most important

(12) Tuttle, O. F. *Geol. Soc. Am. Bull.* **1949**, *60*, 1727–1729.
(13) Mirwald, P. W.; Getting, I. C.; Kennedy, G. C. *J. Geophys. Res.* **1975**, *80*, 1519–1525.
(14) Pruzan, P. *J. Phys. Lett.* **1984**, *45*, L-273–L-278.

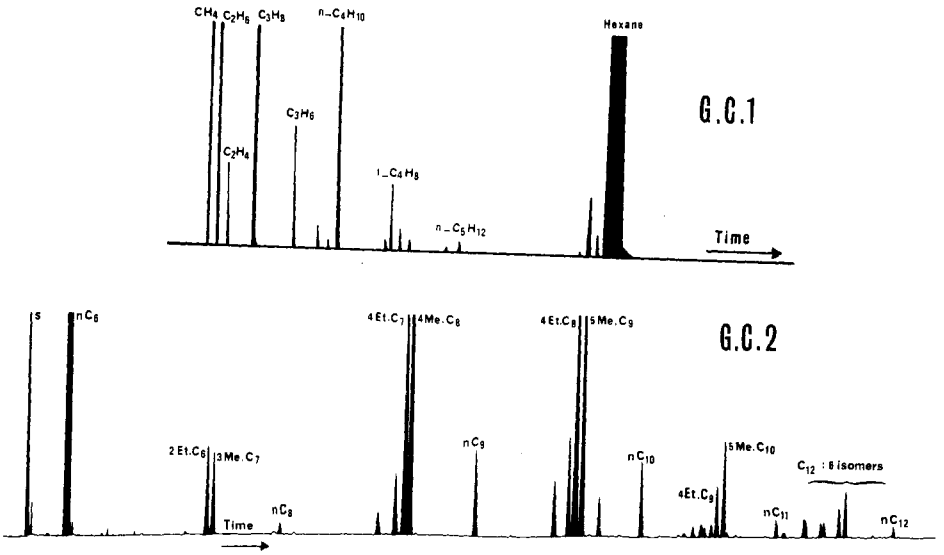

Figure 2. Typical gas chromatogram of the gaseous sample retrieved in the gas ampule (G.C.1) and typical gas chromatogram of the liquid sample retrieved in the cold trap (G.C.2).

Table I. Arrhenius Parameters for Light (C_5^-) Reaction Products Yielded by Least-Squares Fits of Arrhenius Plots of Product Concentration/$[C_6H_{14}]^{1/2}t$

reaction product	log A^a	E, kcal·mol^{-1}	correln coeff
C_2H_6	16.41	68.9	-0.9995
C_3H_8	17.40	72.0	-0.9995
CH_4	13.70	62.9	-0.998
C_3H_6	11.56	56.5	-0.972
1-C_4H_8	14.20	65.0	-0.990
$\sum_1^5 C_nH_{2n+2}$	16.80	69.1	-0.9993
$\sum_2^5 C_nH_{2n}$	12.58	58.9	-0.9797

[a] A is in units of L$^{1/2}$·mol$^{-1/2}$·s^{-1}.

products and for the sum of saturates and unsaturates. These plots required the knowledge of the variations of hexane density with temperature, which are shown in Figure 6. The points at 290 °C also had to be discarded, and the values yielded by least-squares fits of the remaining four points have been reported in Table I. Such a plot could not be done for the sum of C_{12} products, as their concentrations were much too low at the lower temperatures studied to be measured accurately.

Discussion

The pyrolysis of hexane has been the subject of a recent investigation.[15] However, the experimental conditions were very different from those used in the present study: pressure was well below 1 bar, and temperature was above 450 °C. The pyrolysis of other hydrocarbons has also been investigated by numerous authors (see for example Konar et al.,[16] Bull et al.,[17] Baronnet et al.[18]), but all of these studies also involved very low pressures and high temperatures. There is also some limited data on hexadecane pyrolysis at pressures up to 920 bar,[5-7,19,20] but this is also at temperatures above 450 °C.

In all these previous cases, results have been interpretated with free-radical reactions. In the present case, a free-radical reaction mechanism is also proposed, but one should remain aware that due to the unusual pressure and temperature conditions, some qualitative and quantitative

Table II. Mechanism Accounting for the Pyrolysis Products of Hexane in the 210–15600-bar Pressure Range and in the 290–365 °C Temperature Range

Initiation							
C_6H_{14}				→	C_2H_5	+	C_4H_9
C_6H_{14}				→	C_3H_7	+	C_3H_7
C_6H_{14}				→	CH_3	+	C_5H_{11}
Hydrogen Transfer							
CH_3	+	C_6H_{14}	→	CH_4	+	C_6H_{13}[a]	
C_2H_5	+	C_6H_{14}	→	C_2H_6	+	C_6H_{13}[a]	
C_3H_7	+	C_6H_{14}	→	C_3H_8	+	C_6H_{13}[a]	
C_4H_9	+	C_6H_{14}	→	C_4H_{10}	+	C_6H_{13}[a]	
C_5H_{11}	+	C_6H_{14}	→	C_5H_{12}	+	C_6H_{13}[a]	
C_8H_{17}	+	C_6H_{14}	→	C_8H_{18}[a]	+	C_6H_{13}[a]	
C_9H_{19}	+	C_6H_{14}	→	C_9C_{20}[b]	+	C_6H_{13}[a]	
$C_{10}H_{21}$	+	C_6H_{14}	→	$C_{10}H_{22}$[b]	+	C_6H_{13}[a]	
$C_{11}H_{23}$	+	C_6H_{14}	→	$C_{11}H_{24}$[b]	+	C_6H_{13}[a]	
$C_{12}H_{25}$	+	C_6H_{14}	→	$C_{12}H_{26}$	+	C_6H_{13}[a]	
Decomposition							
1-C_6H_{13}				→	C_4H_9	+	C_2H_4
2-C_6H_{13}				→	C_3H_7	+	C_3H_6
3-C_6H_{13}				→	C_2H_5	+	C_4H_8
3-C_6H_{13}				→	CH_3	+	C_5H_{10}
C_3H_7				→	CH_3	+	C_2H_4
C_4H_9				→	C_2H_5	+	C_2H_4
C_5H_{11}				→	C_3H_7	+	C_2H_4
C_8H_{17}				→	radical	+	alkene
C_9H_{19}				→	radical	+	alkene
$C_{10}H_{21}$				→	radical	+	alkene
$C_{11}H_{23}$				→	radical	+	alkene
$C_{12}H_{25}$				→	radical	+	alkene
Isomerization							
for $n \geq 6$							
C_nH_{2n+1}				→	C_nH_{2n+1}		
Addition							
C_6H_{13}	+	C_2H_4	→	C_8H_{17}[a]			
C_6H_{13}	+	C_3H_6	→	C_9H_{19}[b]			
C_6H_{13}	+	C_4H_8	→	$C_{10}H_{21}$[b]			
C_6H_{13}	+	C_5H_{10}	→	$C_{11}H_{23}$[b]			
C_8H_{17}	+	C_4H_8	→	$C_{12}H_{25}$			
C_9H_{19}	+	C_3H_6	→	$C_{12}H_{25}$			
$C_{10}H_{21}$	+	C_2H_4	→	$C_{12}H_{25}$			
Recombination							
C_6H_{13}	+	C_6H_{13}	→	$C_{12}H_{26}$[b]			

[a] Three isomers can be formed. [b] Six isomers can be formed.

(15) Imbert, F. E.; Marshall, R. M. *Int. J. Chem. Kinet.* **1987**, *19*, 81–103.
(16) Konar, R. S.; Purnell, J. H.; Quinn, C. P. *Trans. Faraday Soc.* **1967**, *64*, 1319–1328.
(17) Bull, K. R.; Marshall, R. M.; Purnell, J. H. *Proc. R. Soc. London, A* **1975**, *342*, 259–277.
(18) Baronnet, F.; Dzierzynski, M.; Côme, G. M.; Martin, R.; Niclause, M. *Int. J. Chem. Kinet.* **1971**, *3*, 197–213.
(19) Fabuss, B. M.; Smith, J. O.; Lait, R. I.; Borsanyi, A. S.; Satterfield, C. N. *Ind. Eng. Chem. Process Des. Dev.* **1962**, *1*, 293–299.
(20) Doué, F.; Guiochon, G. *Can. J. Chem.* **1969**, *47*, 3477–3480.

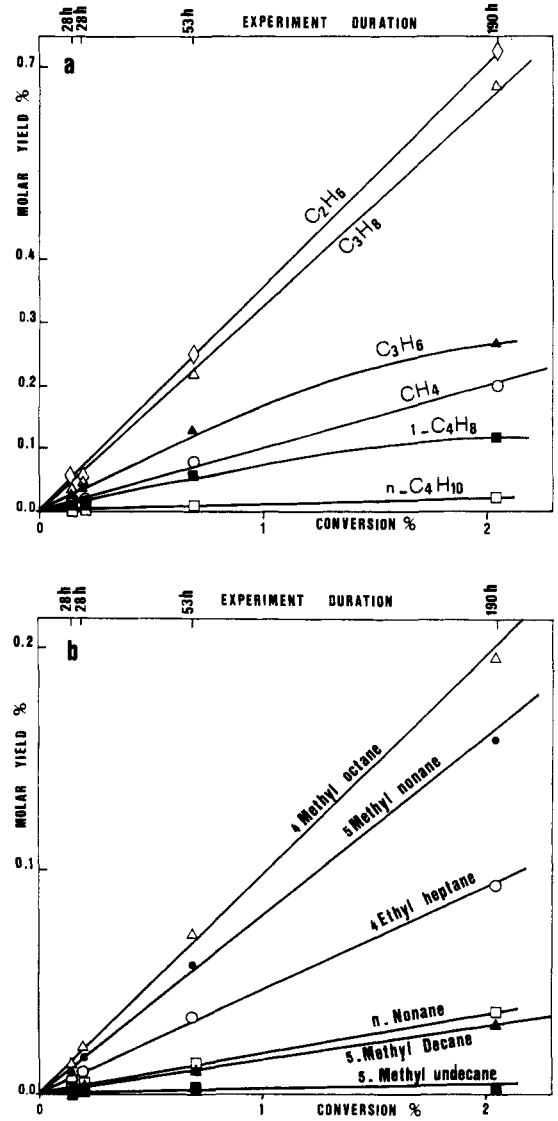

Figure 3. Molar yield (100 × mol of product/initial mol of reactant) of some of the main products versus conversion, at 357 °C and 210 bar: (a) gaseous products; (b) liquid products. To give an idea of the time–conversion relationship, experiment durations are shown (see text).

differences from previous results are to be expected.

(a) Qualitative Aspects. The mechanism proposed here is reported in Table II. Reactions involving free H atoms have not been considered. One reason for this is that the activation energy difference between unimolecular C–C and C–H bond breaking is at least 12 kcal·mol^{-1} for both initiation and decomposition reactions,[21] meaning that in the present temperature range, the rate of C–C bond breaking is at least 10^4 times faster than that for the C–H bond. This is further confirmed by the molecular hydrogen measurements. Indeed, in this case molecular hydrogen can be formed mainly either through a free H atom abstracting another H from a molecule or a radical or by the recombination of two free H atoms. The very low values found for H_2 concentrations clearly show that free H atoms are not important here and that therefore the reactions generating them are sufficiently slow to be neglected. Recent measurements of hydrogen permeability through gold show that, under the present conditions, H_2 does not diffuse through gold.[22]

(21) Allara, D. L.; Shaw, R. *J. Chem. Ref. Data* **1980**, *9*, 523–559.
(22) Chou, I. N. *Am. J. Sci.* **1986**, *286*, 638–658.

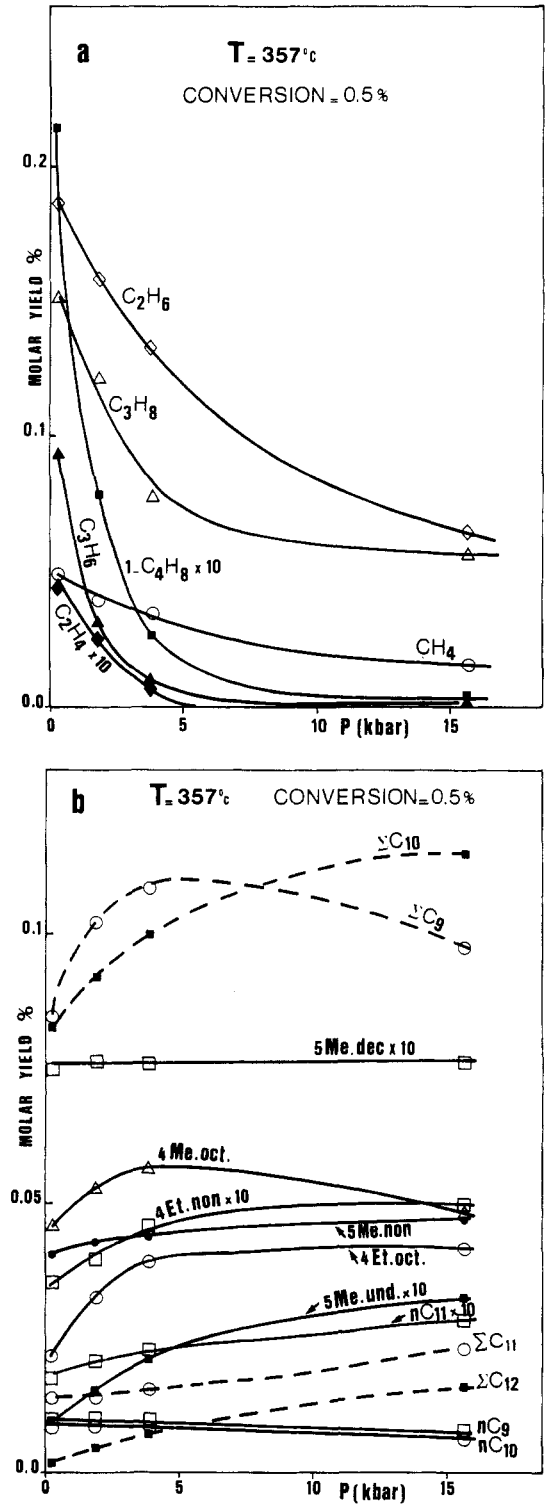

Figure 4. Molar yield (100 × mol of product/initial mol of reactant) of products versus pressure, at 357 °C, at a constant 0.5% conversion. (a) gaseous products; (b) heavy products. The sum of all C_9, C_{10}, etc. are shown.

Light saturates (CH_4, C_2H_6, C_3H_8, n-C_4H_{10}, and n-C_5H_{12}) are products of H-transfer reactions; light unsaturates (C_2H_4, C_3H_6, 1-C_4H_8, and small amounts of 1-C_5H_{10}) are products of decomposition reactions. These compounds are produced by chain reactions, as is observed in the gas phase.[15]

The formation of heavy products (C_6+) can be qualitatively interpreted in two ways: (1) They can be products of recombination reactions; for example, the main three C_9 isomers (4-ethylheptane, 4-methyloctane and n-C_9)

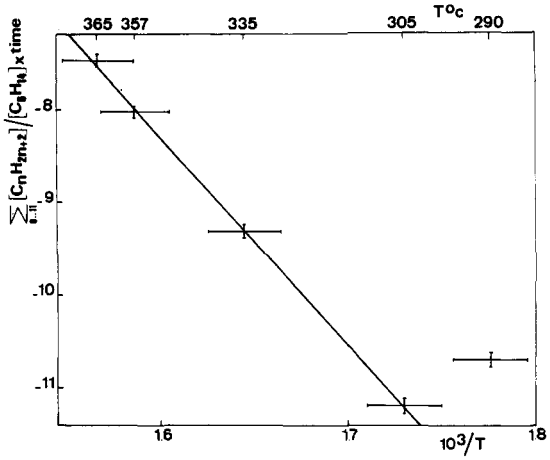

Figure 5. Arrhenius plot of the sum of $\sum[C_nH_{2n+2}]/[C_6H_{14}] \times$ time for n = 8–11, for reaction times of 190 h. If the 290 °C point is discarded (see text), a least-squares fit yields $y = 27.83 + 103.1/4.57T$, with a correlation coefficient of −0.9997.

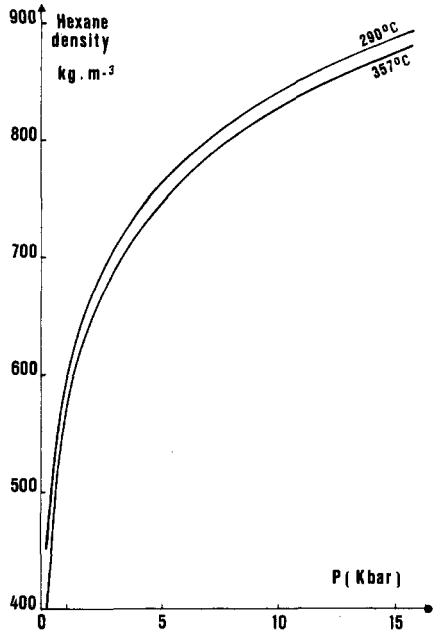

Figure 6. Density of supercritical hexane versus pressure, at 357 and 290 °C, calculated from extrapolated data of Pruzan.[14]

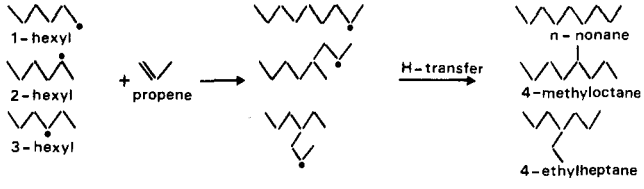

Figure 7. Mechanism of formation of the main three C_9 isomers by addition reactions followed by H-transfer reactions.

could be formed by the recombination of a 1-propyl radical with a 3-hexyl, 2-hexyl, or 1-hexyl radical, respectively. (2) They can be formed by the addition of hexyl radicals on light unsaturates; for example, the formation of the main three C_9 isomers is shown in Figure 7 as resulting from an addition reaction followed by an H-transfer reaction.

As detailed in the following section, only the second possibility (addition reactions) can account for the quantitative observations. The first possibility is of negligible importance. Moreover, the first possibility predicts three C_7, three C_8, three C_9, three C_{10}, three C_{11}, and six C_{12} isomers, while the second one predicts no C_7, three C_8, six C_9, six C_{10}, and six C_{11} isomers (three are formed as shown in Figure 7 and are more important; three are formed by the addition of hexyl radicals to the second carbon of an alkene). Figure 2 clearly shows that the observations are compatible with the second possibility: no C_7 isomers are observed, three C_8 isomers are observed, as well as five C_9 isomers (one peak in the chromatogram is probably made up of two unresolved peaks), six C_{10} isomers, and numerous C_{11} isomers. Some of these numerous C_{11} isomers could also be explained by the addition of secondary C_8+ radicals to unsaturates. The six C_{12} isomers observed here can also be explained by the recombination of hexyl radicals, which predicts six isomers, or by the further addition of heavy radicals to light unsaturates, as shown in Table II. This latter suggestion would also predict that such addition reactions could also readily lead to heavier products. A few experiments were performed at conversions up to 40%, and products of molecular weight up to $C_{16}H_{34}$ were detected. This mechanism of formation of heavy products through addition reactions means that the C_8–C_{12} products shown in Figure 2 are secondary products; Figure 3 implies that they have a pseudoprimary behavior.

Table III. Arrhenius Parameters (after Allara and Shaw[21]) Used for the Reactions of the Simplified Mechanism (See Text)

reaction	log $A^{a,b}$	E, kcal·mol^{-1}	log $K_{357°C}$[a]
I	16.8	82	−11.7
R	11	0	+11
B≈H	9	11	+5.2
−A≈D	13.5	28.5	+3.6
A	8.8	7	+6.4

[a] Units are L·mol^{-1}·s^{-1}. [b] These values have been increased in order to take into account the actual number of reactions for which each reaction of the simplified mechanism stands.

(b) Quantitative Aspects. The detailed quantitative treatment of the present reaction mechanism is not feasible by an analytical method, as the equations that would have to be written cannot be solved. Computer modeling, which is not performed at this point, would be necessary. However, if a simplified mechanism is used, which consists of a small number of reactions whose rate constants are derived from the literature, some quantitative implications of this mechanism can be tested against the experimental results. This simplified mechanism is

$$C_6H_{14} \rightarrow 2C_3H_7 \quad \text{(I)}$$

$$C_3H_7 + C_6H_{14} \rightarrow C_3H_8 + C_6H_{13} \quad \text{(H)}$$

$$C_6H_{13} \rightarrow C_3H_6 + C_3H_7 \quad \text{(D)}$$

$$C_6H_{13} + C_3H_6 \rightarrow C_9H_{19} \quad \text{(A)}$$

$$C_9H_{19} + C_6H_{14} \rightarrow C_9H_{20} + C_6H_{13} \quad \text{(B)}$$

$$C_9H_{19} \rightarrow C_6H_{13} + C_3H_6 \quad \text{(−A)}$$

$$2C_6H_{13} \rightarrow C_{12}H_{26} \quad \text{(R)}$$

Thus, each type of reaction and each type of product is represented here: C_3H_8 stands for light saturates, C_3H_6 stands for light unsaturates, C_9H_{20} stands for heavy C_8–C_{11} products, and $C_{12}H_{26}$ stands for recombination products. To perform calculations, knowledge of the rate constants of the above reactions is necessary. These rate constants have not been measured at the high pressures involved here. However, their values or those of similar reactions are known in the gas phase,[21] and it is assumed here that these gas-phase values can also be used here with a reasonably small error at 210 bar.

One must keep in mind that each of the above reactions actually stands for several reactions. Their rate constants

Table IV. Comparison of Experimental Values Obtained at 210 bar with Those Predicted by Equations Deduced from the Simplified Mechanism (See Text)

	predicted for $t \approx 10^3$ s			experimental $t = 10^{5.8}$ s			predicted for $t \approx 10^7$ s		
	log A^a	E^b	log $K_{357°C}{}^a$	log A^a	E^b	log $K_{357°C}{}^a$	log A^a	E^b	log $K_{357°C}{}^a$
light saturates C_3H_8, etc.	16.4	69.5	−7.7	16.8	69.1	−7.2	16.4	69.5	−7.7
light unsaturates C_3H_6, etc.	16.4	69.5	−7.7	12.6	58.9	−7.8	4.7	21.5	−2.8
C_8–C_{11}	28.4 + log t	117.5	−12.7 + log t	27.8	103.1	−8.0	16.1	69.5	−8.1
C_{12}	16.8	82	−11.7	c	c	−9.9	16.8	82	−11.7

[a] Units are L, mol, and s, with appropriate exponent: see Table I and Figure 5. [b] Units of kcal·mol^{-1} [c] Not measured.

must then account for this: their values, reported in Table III, are slightly higher than those found in the literature.[21] For example, the decomposition rate constant has an A factor of 13.5 instead of the literature value of 13.2 because this reaction also stands for the decompositions yielding butene and ethylene.

It is now possible to use this mechanism to calculate the predicted rates of formation of each class of products and then to compare them to the experimental values obtained for the sum of light saturates, light unsaturates, and C_8–C_{11} products. For convenience, C_3H_7, C_6H_{13}, and C_9H_{19} radicals will be referred to as R, M, and N, respectively. If a steady state is assumed, expressions for radical concentrations can be obtained. Initiation and recombination rates being equal, the concentration of M can be written as

$$[M] = (K_I[C_6H_{14}]/K_R)^{1/2} \quad (1)$$

similarly

$$[R] = 2K_I/K_H + (K_D/K_H)(K_I/[C_6H_{14}]K_R)^{1/2} \quad (2)$$

and

$$[N] = K_A(K_I[C_6H_{14}]/K_R)^{1/2}[C_3H_6]/(K_B[C_6H_{14}] + K_{-A}) \quad (3)$$

Numerical expressions for these expressions are highly desirable. By using the values of Table III and assuming that, at low conversion, reaction products do not modify hexane density in an important manner, we get

$$\log [M] = -11 \quad (4)$$

$$\log [R] = -13.3 \quad (5)$$

$$\log [N] = -10.5 + \log [C_3H_6] \quad (6)$$

Concentration units are mol·L^{-1}. These values justify the choice of the recombination reactions used here and in Table II, where two hexyl radicals recombine. Indeed, from Figure 3, the concentrations of light unsaturates do not exceed 0.02 mol·L^{-1} and the concentration of N radicals should then be much smaller than those of M radicals.

These values also predict that the addition of R to propene is negligible. Had this not been so, some heptane isomers would have been detected, as resulting, for example, from the addition of 1-butyl to propene or of 1-propyl to butene.

The rate of recombination is given by

$$d[C_{12}H_{26}]/dt = K_I[C_6H_{14}] \quad (7)$$

Table III shows that the first term in eq 2 is negligible, and thus

$$d[C_3H_8]/dt \approx K_D(K_I[C_6H_{14}]/K_R)^{1/2} \quad (8)$$

The C_3H_6 concentration is found by solution of a simple differential equation. From Table III, eq 6, and what has been said about C_3H_6 concentrations, the rate of reaction −A can be neglected and we get

$$[C_3H_6] \approx (K_D/K_A)(1 - \exp(-K_A[M]t)) \quad (9)$$

This expression lends itself to simple calculations in only two distinct cases. In case 1, $t \ll 1/K_A[M]$. Typically, $t \approx 1000$ s. We then have

$$d[C_9H_{20}]/dt \approx d[C_3H_8]/dt \approx K_D(K_I[C_6H_{14}]/K_R)^{1/2} \quad (10)$$

and if reaction −A is neglected

$$d[C_9H_{20}]/dt \approx K_AK_DK_I[C_6H_{14}]t/K_R = K_A[M][C_3H_6] \quad (11)$$

In case 2, $t \gg 1/K_A[M]$. Typically, $t \approx 10^7$ s. Then C_3H_6 reaches a steady concentration

$$[C_3H_6] \approx K_D/K_A \quad (12)$$

and therefore, with −A still neglected

$$d[C_9H_{20}]/dt \approx K_D(K_I[C_6H_{14}]/K_R)^{1/2} \quad (13)$$

It must be pointed out here that while eq 13 predicts a linear dependence of heavy product yields on time, once unsaturates have reached a steady concentration, eq 11 predicts that at low conversion, heavy product yields should increase linearly with the square of time, which is not observed in Figure 3b. At least two factors can account for this. (a) Although straight lines have been drawn in Figure 3b, it can be observed that the first three points obtained do show a slightly nonlinear increase with conversion, which could be attributed to a dependence on the square of conversion (or time). However, it is clear that this is within the experimental error and that insufficient data are available to make precise deductions about the second derivative of the yields plotted here. (b) Data available in the literature[21] show that the pyrolysis rate is faster for branched alkanes than for linear ones. These heavy products are mainly branched ones, and therefore their pyrolysis, which should be faster than that of hexane, should attenuate the expected curvature of the plots of Figure 3b. However, it is not possible here to determine whether these two factors account quantitatively for the apparent discrepancy between the measured and predicted variations in heavy products yields with time.

Another point is that it can readily be checked from the values of Table III and from eq 4 and 5 that, at both short ($t \approx 10^3$s) and long ($t \approx 10^7$s) reaction times, the formation of C_9H_{20} through the recombination of R and M radicals is indeed negligible: these reactions do not contribute to the formation of C_8–C_{11} products in an important manner after a reaction time of about 1 min.

It is now possible to compare the numerical values yielded by eq 7, 8, 10, 11, 12, and 13 to the experimental results obtained at 210 bar for each class of products, as reported in Table I and Figure 5. This comparison is shown in Table IV. Predicted values are (d[products]/dt)$[C_6H_{14}]^{1/2}$ for C_5− products and (d[products]/dt)$[C_6H_{14}]$ for C_8+ products so that these values can be compared directly to the experimental ones. The experimental results are for a reaction time of about $10^{5.8}$ s, which is in between the values for both cases where calculations have been performed. However the values of the rates of for-

Table V. Predicted Effect of Pressure on the Rate of Formation of Each Type of Product at Constant Reaction Time, at 357 °C

	log (concentration at 15 600 bars/concentration at 210 bars)					
	short reaction time			long reaction time		
	due to density	due to ΔV^*	resulting effect	due to density	due to ΔV^*	resulting effect
light saturates	+0.2	−2	−1.8	+0.2	−2	−1.8
light unsaturates	+0.2	−2	−1.8	0	−2	−2
C_8–C_{11}	+0.4	−2	−1.6	+0.2	−2	−1.8
recombination products	+0.4	−1	−0.6	+0.4	−1	−0.6

mation of products certainly shift from the lower to the higher conversion values in a continuous manner, and if the mechanism is correct, the experimental results should fall in between the values predicted by these two cases.

Indeed, Table IV clearly shows that for light unsaturates and for C_8–C_{11} products the experimental values do fall within the predicted range. Also the values measured for light saturates are very close to the calculated ones, which do not vary with time. Rate parameters could not be measured for $C_{12}H_{26}$ products (formed through recombination reactions, according to the simplified mechanism), but when one considers their rate constant at 357 °C, a major discrepancy appears and it is clear that recombination reactions account for only 1% of the observed $C_{12}H_{26}$ yield at 210 bar. The presence of addition reactions of N radicals on unsaturates has to be taken into account to explain the observations.

This section shows that, even though some approximations had to be made, the proposed mechanism with chain reactions followed by addition reactions can account with a reasonable accuracy for the qualitative and quantitative results obtained at 210 bar. Since the same products are qualitatively present at pressures up to 15 600 bar, it is a reasonable suggestion that the same reactions take place. The purpose of the next section is to attempt to understand the variation of products relative yields with pressure.

(c) Effect of Pressure. High pressure has mainly three effects. (1) It increases the viscosity of hexane, thus retarding bimolecular reactions by hindering the migration of reacting molecules or radicals[23] (cage effect). Unfortunately, to my knowledge, there are no data on the viscosity of hexane in the conditions studied. Moreover, it is likely that the small amounts of argon present in the reactor considerably lower hexane viscosity, keeping it well below the point where reactions become diffusion controlled. The temperatures involved are also probably too high to allow large viscosity values at 15 600 bar. Clearly this point is highly speculative at present, but it is assumed in this case that radical diffusion is not a limitating factor.

(2) It increases the density of hexane. As shown in Figure 6, at 357 °C, hexane density more than doubles between 210 and 15 600 bar. For short reaction times, according to eq 8, 10, and 11, this should relatively favor the formation of heavy products, whose rate depends on hexane concentration, while the rate of formation of light products is proportional to the square root of the concentration. This is qualitatively observed in Figure 4.

(3) It modifies rate constants, K, according to the following relationship:

$$\left(\frac{\partial \ln K}{\partial P}\right)_T = \frac{-\Delta V^*}{RT} \qquad (14)$$

where ΔV^* is the activation volume, as defined in the transition state theory. ΔV^* is negative for bimolecular reactions, here recombination, addition, and H-transfer reactions. Their rate constants shall therefore increase with pressure. ΔV^* is positive for unimolecular reactions, here initiation and decomposition reactions, whose rate constant shall decrease with pressure.

Typically, at 357 °C, a reaction with an activation volume of 8 $cm^3 \cdot mol^{-1}$ will see its rate constant vary by a factor of 10 over the pressure range investigated here. Also, eq 14 shows that the effect of pressure is going to be less apparent at high temperature, which means that a pressure range wider than that relevant to geochemical processes has to be investigated at 357 °C if one wishes to have an idea of the effects of pressure at the lower temperatures of geochemical interest, that is, below 200 °C.[9]

Unfortunately, values of the activation volumes of the reactions involved here are not available in the literature. However, values of the activation volumes of related reactions can be found in the literature (see for example Isaacs[24]), and it is reasonable to assume an activation volume of +8 $cm^3 \cdot mol^{-1}$ for unimolecular reactions and an activation volume of −8 $cm^3 \cdot mol^{-1}$ for bimolecular reactions.

Table V sums up the effects of a pressure increase from 210 to 15 600 bars on the rate of formation of each type of product at 357 °C, as predicted by eq 7, 8, 10, 11, 12, and 13. It is important to stress here the approximate character of such an evaluation. Indeed, unlike the values of the rate constants used earlier at low pressure, the error in estimating the activation volumes can lead to errors of 1 power of 10 or more in the data of Table V. However, from reading Table V, one would expect to see the overall reaction rate decrease by almost 2 orders of magnitude. This effect has been found to be within experimental error. But again, it should be remembered that the experimental problems encountered, mainly in the temperature measurements, are very severe. Also, the 15 600-bar experiments were performed in an apparatus very different from the one used for the other experiments. This apparatus was in another laboratory, which made the accurate intercalibration of the temperature measurements all but impossible. This, combined with the inaccurate values of the activation volumes, may explain why this predicted effect could not be observed.

However, earlier work on hexadecane pyrolysis between 1 and 920 bar,[6] although performed at temperatures higher than in the present work, shows that the overall rate constant of hexadecane pyrolysis does decrease between about 200 and 920 bar, which may support the present prediction.

Table V also predicts that the relative yield of heavy products at constant conversion should increase with pressure. Consequently, relative light product yields should decrease, as is observed in Figure 4. That the yield of unsaturates decreases much more than that of light saturates could be explained by activation volumes different from ±8 $cm^3 \cdot mol^{-1}$. For example, if the activation volumes of addition reactions were lower than −8 $cm^3 \cdot mol^{-1}$,

(23) Hamann, S. D. *Trans. Faraday Soc.* **1958**, *54*, 507–511.

(24) Isaacs, N. S. *Liquid Phase High Pressure Chemistry*; J. Wiley and Sons: New York, 1981; Chapter 4.

then, for short reaction times, the relative yield of C_8-C_{11} products would decrease more with pressure than predicted by Table V. Also, for long reaction times, the relative yield of light unsaturates would decrease more with pressure than predicted by Table V.

Both of these effects, which are implied by a lower addition activation volume, are observed in Figure 4, as these results were obtained for a reaction time that, as detailed earlier, is intermediate between what is here called "short" and "long". It is then likely that these activation volumes are lower than -8 $cm^3 \cdot mol^{-1}$.

Another effect of high pressure predicted by Table V is that the rate of formation of recombination products increases by about a power of 10 relative to other rates. It is then possible that, at high pressure, recombination rates are not negligible. This could explain the large increase in $C_{12}H_{26}$ products observed in Figure 4.

Conclusion and Geochemical Implications

The mechanism of hexane pyrolysis under the present low-temperature–high-pressure conditions is very different from what has been described under the more often studied high-temperature–low-pressure conditions.[15] Under those conditions, at similar conversion, hexyl radicals through one or more decomposition reactions yield one or more olefins and a light alkane. In the present conditions, where collisions are much more frequent, hexyl radicals, besides decomposing unimolecularly, can also bimolecularly add to alkenes to yield heavy radicals, which lead to large amounts of heavy products. As pressure is increased, these bimolecular reactions are relatively favored, while decomposition rates show a relative decrease.

Another way of saying this is, if one considers the simplified mechanism used earlier, that, in the gas phase, hexane pyrolysis is mainly accounted for by stoichiometries of the type

$$C_6H_{14} \rightarrow C_3H_6 + C_3H_8$$

while, at high pressure, other stoichiometries such as

$$2C_6H_{14} \rightarrow C_3H_8 + C_9H_{20}$$

appear. The rates of these latter stoichiometries increase relative to the rates of the former when presure is increased.

These results clearly demonstrate the important influence of pressure and temperature on the product distribution of hexane pyrolysis. These influences should be taken into account when modeling geochemical systems. Computer simulations of the present work are under way. They will yield numeric values of kinetic parameters and of their pressure dependence (activation volumes), which will allow the extrapolation of these results down to the temperature range in which petroleum actually evolves (80–200 °C according to Tissot and Welte[9]). However, a tremendous amount of work still has to be performed before the present data can be applied to the complex mixtures of geochemical interest, which are also made up of branched, cyclic, and aromatic hydrocarbons and also contain molecules with heteroatoms, mainly sulfur, oxygen, and nitrogen. Considering the scarcity of the data, it is a bit presumptuous to speculate on the effect of high pressure on these other chemical structures. However, it is well-known that the presence of heteroatoms results in weaker bonds. A recent study of the gas-phase pyrolysis of dimethyl sulfide[25] shows that C–S bonds break more easily (74 $kcal \cdot mol^{-1}$) than C–C bonds (82 $kcal \cdot mol^{-1}$), resulting in an overall activation energy in the 400–450 °C range of only 47 $kcal \cdot mol^{-1}$, as opposed to the higher value of 58 $kcal \cdot mol^{-1}$ found for hexadecane pyrolysis[7] under similar physical conditions. These values can be related to the observations of Henderson and Weber,[26] who measured overall activation energy for the thermal degradation of a variety of crude oils between 260 and 371 °C and found values ranging from 43.6 to 62.2 $kcal \cdot mol^{-1}$, the higher values being those obtained for the most paraffinic oils.

It can therefore be speculated that heteroatom-containing molecules are going to be very reactive ones. The same can be predicted of alkyl-substituted aromatic hydrocarbons, as βC–C fission only requires about 67 $kcal \cdot mol^{-1}$.[27] It is then possible that the composition of a crude oil will considerably affect its high-pressure thermal degradation. However, it is likely that the effects observed in the present work will also be qualitatively observed for complex mixtures, as the same types of free-radical reactions are to be expected, which would result in a competition between unimolecular and bimolecular reactions.

Other chemical factors such as the presence of nonhydrocarbon fluids, surface effects, and mineral catalysis can also take place in natural settings, which could modify the above results in a yet unknown manner. Also, physical factors such as the opening of the system and the migration of the lighter reaction products, as well as long reaction time resulting in large extents of conversion, could render the effects evidenced in this study difficult to observe in geological systems. Clearly, much more data is needed before all these aspects of the geological thermal evolution of organic matter are understood in a satisfactory manner.

Acknowledgment. Analytical advice throughout this research by F. Behar and co-workers is greatly appreciated. Experimental advice for high-pressure experimentation by B. Goffé was extremely helpful. Experiments at 15 600 bars were performed by C. Chopin in Professor W. Schreyer's Institut für Mineralogie, Ruhr Universität, Bochum, Federal Republic of Germany. Mass spectrometry facilities and advice were provided by N. Morin and C. Rolando. Molecular hydrogen was measured by F. Pineau. Numerous discussions with F. Baronnet, G. Scacchi, and co-workers prooved very fruitful. I also thank the reviewers and T. R. Hughes for their interesting comments.

Registry No. C_6H_{14}, 110-54-3; C_2H_6, 74-84-0; C_3H_8, 74-98-6; CH_4, 74-82-8; C_3H_6, 115-07-1; C_4H_8, 106-98-9.

(25) Shum, L. G. S.; Benson, S. W. *Int. J. Chem. Kinet.* **1985**, *17*, 749–761.

(26) Henderson, J. H.; Weber, L. *J. Can. Pet. Technol.* **1965**, *4*, 206–212.

(27) Savage, P. E.; Klein, M. T. *Prepr.—Am. Chem. Soc., Div. Pet. Chem.* **1985**, *30*, 642–651.